

# Physics with the ALICE experiment

Yuri Kharlov, for the ALICE collaboration<sup>1</sup>

<sup>1</sup>*Institute for High Energy Physics, Protvino, 142281 Russia*

ALICE experiment at LHC collects data in pp collisions at  $\sqrt{s}=0.9, 2.76$  and 7 TeV and in PbPb collisions at 2.76 TeV. Highlights of the detector performance and an overview of experimental results measured with ALICE in pp and AA collisions are presented in this paper. Physics with proton-proton collisions is focused on hadron spectroscopy at low and moderate  $p_t$ . Measurements with lead-lead collisions are shown in comparison with those in pp collisions, and the properties of hot quark matter are discussed.

## 1. INTRODUCTION

ALICE is a dedicated experiment built to exploit the unique physics potential of heavy-ion interactions at LHC energies [1]. Properties of strongly interacting matter at extreme energy density are explored via a comprehensive studies of hadron, muon, electron and photon production in the collisions of heavy nuclei and their comparison with proton-proton collisions.

Presently, the ALICE collaboration consists of about 1600 members from 33 countries. Russian nuclear-physics community takes an active part in ALICE since the very beginning, now counting 134 members from 12 institutes. Russian institutes contribute in almost every major sub-detectors of the ALICE experiment, and also take part in physics analysis of data collected in 2010–2011.

The ALICE experiment has collected a rich sample of data with proton-proton and lead-lead collisions. In 2010 and beginning of 2011, about  $10^9$  events with the minimum bias trigger were recorded, corresponding to the integrated luminosity  $\int \mathcal{L}dT = 16 \text{ nb}^{-1}$ . Rare-event triggers on muons, jets and photons were dominant in data taking with the proton beams at collision energy  $\sqrt{s} = 7 \text{ TeV}$  in the second half of 2011, with the delivered integrated luminosity  $\int \mathcal{L}dT = 4.9 \text{ pb}^{-1}$ . Limited data samples with the proton beams at collision energies  $\sqrt{s} = 0.9$  and 2.76 TeV have been also recorded with integrated luminosities  $\int \mathcal{L}dT = 0.14$  and  $1.3 \text{ nb}^{-1}$  respectively.

Among rare-event triggers used in data taking in 2011, one has to mention the trigger on the MUON detector selecting events with muons in the high-rapidity range to enrich statistics for  $J/\psi$  and  $\Upsilon$  signals (this trigger was in operation since 2010). A trigger based on the electromagnetic calorimeter (EMCAL) was selecting events with high-energy photons and jets in the central barrel. Another ALICE calorimeter, a photon spectrometer PHOS, has provided a trigger on photons with a moderate energy threshold, to enhance a data sample for neutral meson and direct photon studies.

The first run with lead-lead beams at collision energy  $\sqrt{s_{NN}} = 2.76$  TeV was taken with ALICE in November 2010. The delivered integrated luminosity was  $\int \mathcal{L} dT = 10 \mu\text{b}^{-1}$ . The dominant trigger in 2010 was a minimum bias one. In November 2011, the LHC has delivered 10 times more data, and the ALICE experiment has restricted the minimum-bias trigger share in favor of several rare-event triggers with the total life time 80%. Detector VZERO has deployed triggers on the most central events with selected centralities 0 – 10% and semi-central events with centralities 20 – 60%. A trigger on ultra-peripheral collisions was realized on SPD and TOF detectors. Other triggers implemented earlier in pp collisions on EMCAL, PHOS and MUON detectors, were also active in the PbPb run 2011.

## 2. HADRON PRODUCTION IN PROTON-PROTON COLLISIONS

Measurements of identified hadron spectra are considered as an important test of various non-perturbative models of hadron production at high energies, as well as those of perturbative QCD calculations. ALICE performs extensive studies of hadron production due to its powerful particle identification capabilities [1]. Charged particles are identified by several tracking detectors covering complimentary kinematic ranges. Barrel tracking detectors are embedded into a solenoidal magnet with magnetic field of 0.5 T. This is a relatively soft magnetic field which allows to reconstruct charged tracks at transverse momenta starting from  $p_t > 50$  MeV/ $c$ . Inner Tracking System (ITS) and Time Projection Chamber (TPC) can identify charged particles in the full  $2\pi$  azimuthal angle and pseudorapidity range  $|\eta| < 0.9$ , via measurements of their ionization loss  $dE/dx$ . Time-of-flight measurements, provided by the TOF detector in the same solid angle as ITS and TPC, can discriminate charged pions, kaons and protons in a higher momentum range. The limited-acceptance High-Momentum Particle Identification detector (HMPID) is a Cherenkov detector covering a solid angle

$\Delta\phi = 60^\circ$  and  $|\eta| < 0.6$  is used to identify charged particles at a higher momentum range, up to  $p = 5 \text{ GeV}/c$ . Transition Radiation Detector (TRD) is another barrel detector surrounding TPC, which is designed to identify electrons and at present covers about a half of the complete azimuthal angle.

Photons and neutral mesons decaying into photons are detected and identified by two electromagnetic calorimeters. A precise Photon Spectrometer (PHOS) is a high-granularity calorimeter built of lead tungstate crystals ( $\text{PbWO}_4$ ). Its small Molière radius, high density and high light yield allow to detect photons with the best possible energy resolution in the energy range up to  $E < 100 \text{ GeV}$  in the azimuthal angle range  $\Delta\phi = 60^\circ$  and  $|\eta| < 0.13$ . Its high spatial resolution provides measurements of neutral pions via invariant mass spectrum at transverse momenta  $0.6 < p_t < 50 \text{ GeV}/c$ . Another, wide-aperture Electromagnetic Calorimeter (EMCAL) is a sampling-type calorimeters built of lead-scintillator modules. Its primary goal is to trigger jets and measure a neutral component of jets. Dynamic range of EMCAL covers energies up to  $250 \text{ GeV}$ , and granularity of this calorimeter allows to reconstruct  $\pi^0$  mesons at transverse momenta  $1 < p_t < 20 \text{ GeV}/c$ .

Muon identification is provided in ALICE by the muon arm which is installed in the forward rapidity range  $2.5 < y < 4$ . This muon detector is a magnet spectrometer consisting of a set of proportional chambers in the dipole magnetic field. Hadronic background is suppressed by the hadron absorber installed in front of the muon spectrometer.

Using charged hadron identification in ITS, TPC and TOF, ALICE has measured production spectra  $dN/dp_t$  of identified charged hadron ( $\pi^\pm$ ,  $K^\pm$ ,  $p$ ,  $\bar{p}$ ) in the minimum bias pp collisions at collision energies  $\sqrt{s} = 0.9$  [2] and  $7 \text{ TeV}$  [3] (Fig.1). The spectra were fitted with the Tsallis function [4]

$$E \frac{d^3\sigma}{dp^3} = \frac{\sigma_{pp}}{2\pi} \frac{dN}{dy} \frac{c \cdot (n-1)(n-2)}{nC [nC + m(n-2)]} \left(1 + \frac{m_t - m}{nC}\right)^{-n}, \quad (1)$$

where the fit parameters are  $dN/dy$ ,  $C$  and  $n$ ,  $\sigma_{pp}$  is the proton-proton inelastic cross section,  $m$  is the meson rest mass and  $m_t = \sqrt{m^2 + p_t^2}$  is the transverse mass. The integrated yield at  $y = 0$ , defined by the Tsallis parameter  $dN/dy$ , was evaluated from the ALICE data, and thus the total yields of charged pions, kaons and protons was found. The ratios of integrated yields  $K^\pm/\pi^\pm$ ,  $\bar{p}/\pi^-$  and  $p/\pi^+$  in pp collisions at  $\sqrt{s} = 0.9$  and  $7 \text{ TeV}$  were compared with those measured at lower collision energies, as shown in Fig.2. A trend of slight increase of  $K^\pm/\pi^\pm$  ratio with  $\sqrt{s}$  can be observed. ALICE data also suggest that baryon-antibaryon

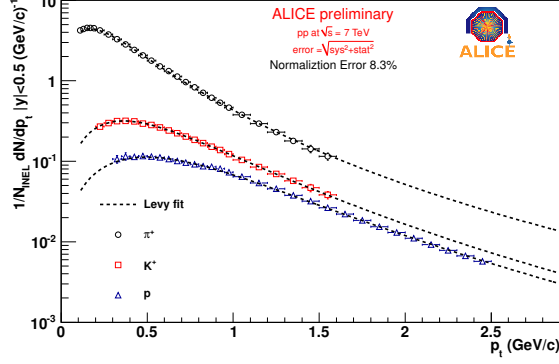


**Figure 1.** Transverse momentum spectra of  $\pi^-$ ,  $K^-$ ,  $\bar{p}$  in pp collisions at  $\sqrt{s} = 7$  TeV. The lines are the Levy-Tsallis fits.

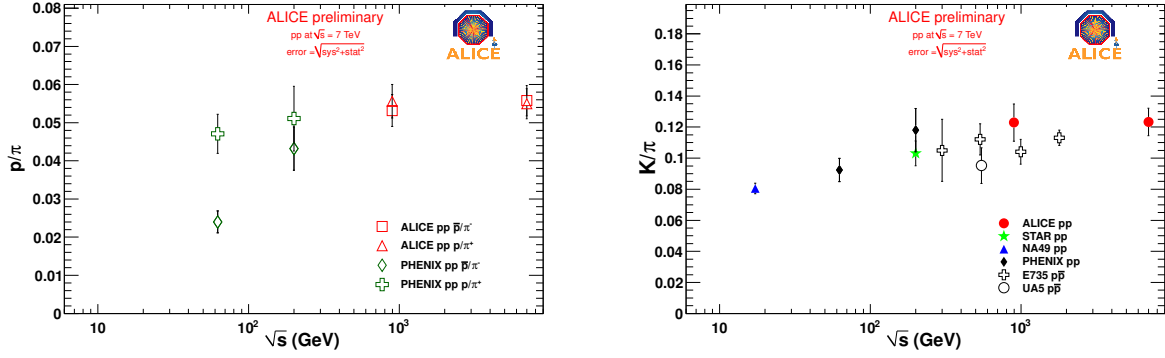


**Figure 2.** Integrated yield ratio of  $K/\pi$  (left) and  $\bar{p}/\pi^-$  (right) as a function of collision energy.

asymmetry, observed at RHIC, vanishes at LHC energies, as expected.

Tsallis parameterization allows to find also the mean transverse momentum  $\langle p_t \rangle$  and to observe its evolution with collision energy (Fig.3). Comparison of mean  $p_t$  of different hadron species measured at different collision energies indicates that hadron production spectra become harder at higher  $\sqrt{s}$ , and also mean  $p_t$  grows with hadron mass.

ALICE has also measured production spectra of neutral pions and  $\eta$  mesons in pp collisions at  $\sqrt{s} = 0.9, 2.76$  and  $7$  TeV, using the Photon Spectrometer (PHOS) for real photon detection and central tracking system for converted photon reconstruction [5]. Neutral meson reconstruction, performed via invariant mass spectra of photon pairs, allowed to measure differential cross section of  $\pi^0$  and  $\eta$  in a wide  $p_t$  range. In particular, the spectrum of  $\pi^0$  production at the three collision energies are shown of the left plot of Fig.4. Hadron production at high  $p_t$  can be well calculated in the next-to-leading orders of perturbative QCD

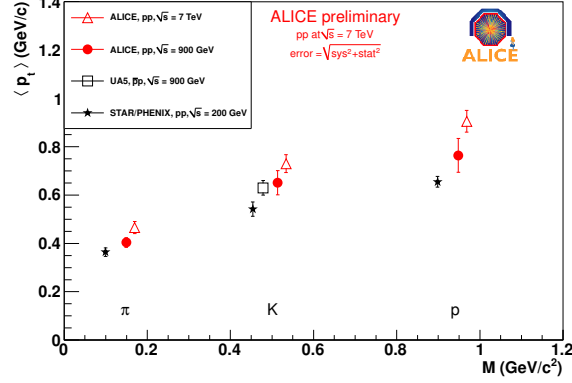


**Figure 3.** Mean  $p_t$  for charged  $\pi$ ,  $K$  and  $p$  at different collision energy in pp collisions.

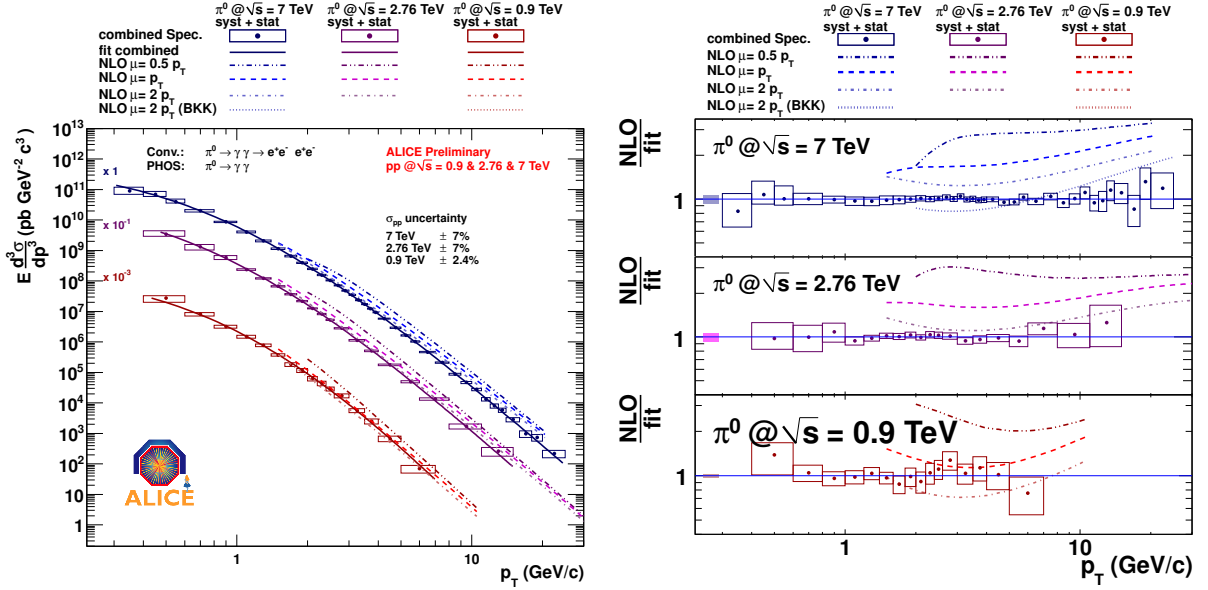


**Figure 4.** Production spectrum of  $\pi^0$  in pp collisions at  $\sqrt{s} = 0.9, 2.76$  and  $7$  TeV (left) and ratio of NLO pQCD calculations to the measured spectra (right).

(NLO pQCD). These calculations are based on parton distribution (PDF) and fragmentation functions (FF) measured at lower energies. Application of those PDF's and FF's to the new energy domain delivered by LHC, lead to extrapolations of those functions to the kinematic region where the functions have large uncertainties. The ratio of differential cross sections of  $\pi^0$  and  $\eta$  mesons in pp collisions, calculated by NLO pQCD, to the Tsallis fit of the ALICE measurements are shown by curves on the right plot of Fig.4. Data points on this plot represent the ratio of the measured cross section to the Tsallis fit to the measurement, which demonstrates the quality of the data description by the Tsallis parameterization. This

comparison of theoretical calculations and experimental measurements demonstrates that NLO pQCD at the QCD scale  $\mu = p_t$  describes well hadron production in pp collisions at  $\sqrt{s} = 0.9$  TeV, while significantly overestimate it at  $\sqrt{s} = 7$  TeV. No common set of pQCD parameters can be found to describe equally well the spectra of pion production at all three collision energies.

Strangeness production is one of the most important observables for studying the strongly interacting matter produced in heavy-ion collisions. That is why measurements of complete set of strange hadrons in pp collisions is necessary as a reference for comparison with heavy ion collisions. Besides charged kaons mentioned earlier, ALICE has measured production spectra of many other strange hadrons, as well as those of mesons with hidden strangeness ( $K^*$ ,  $\Lambda$ ,  $\Sigma$ ,  $\Omega$ ,  $\phi$  and strange resonance baryons). Production yields of  $(\Sigma^* + \bar{\Sigma}^*)/2$  and  $\phi$  mesons in pp collisions at  $\sqrt{s} = 7$  TeV are shown in Fig.5 and are compared with several MC predictions.

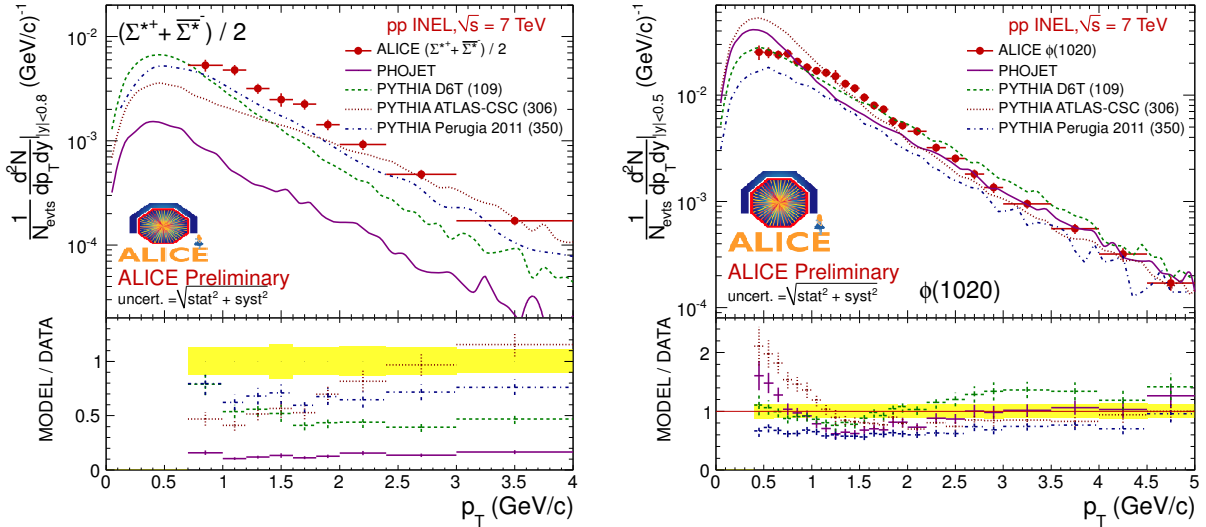


**Figure 5.** Production spectrum of  $(\Sigma^{*+} + \bar{\Sigma}^{*-})/2$  and  $\phi$  in pp collisions at  $\sqrt{s} = 7$  TeV with Monte Carlo predictions by different models.

Identified hadron spectra measured at LHC energies, in conjunction with spectra measured by previous experiments at lower collision energies, allow to observe evolution of hadron production properties with  $\sqrt{s}$ . Predictions of various phenomenological models, as well as NLO pQCD calculations were found to be unable to describe all identified hadron spectra measured by ALICE in pp collisions

### 3. HEAVY ION COLLISIONS

Analysis of the first heavy-ion data collected in 2010 brought many results giving an insight into the properties of strongly interacting matter at the new energy density regime. Observables characterizing this matter are classified into several groups which will be reviewed in this section.

#### 3.1. Global event properties

As heavy nuclei are extended objects, centrality determination is an essential point for all heavy-ion measurements. Centrality of the collision, directly related to the impact parameter and to the number of nucleons  $N_{\text{part}}$  participating in the collision, allows to study particle production versus the density of the colliding system. In the ALICE experiment, collision centrality can be measured by several detectors. The best accuracy of centrality measurement is achieved with the scintillator hodoscope VZERO covering pseudorapidity ranges  $2.8 < \eta < 5.1$  and  $-3.7 < \eta < -1.7$ . Distribution of the sum of amplitudes in VZERO in minimum bias Pb-Pb collisions is shown in Fig.6 (left) [6]. Centrality classes were defined by Glauber model, and the fit of the Glauber model to the data is shown by a solid line in this plot. Centrality resolution for all the estimators can be found in Fig.6 (right) [7] which demonstrates that the best resolution is achieved with the VZERO detector, and is equal to about 0.5% in the most central events, and varies up to 1.5% in the most peripheral collisions.

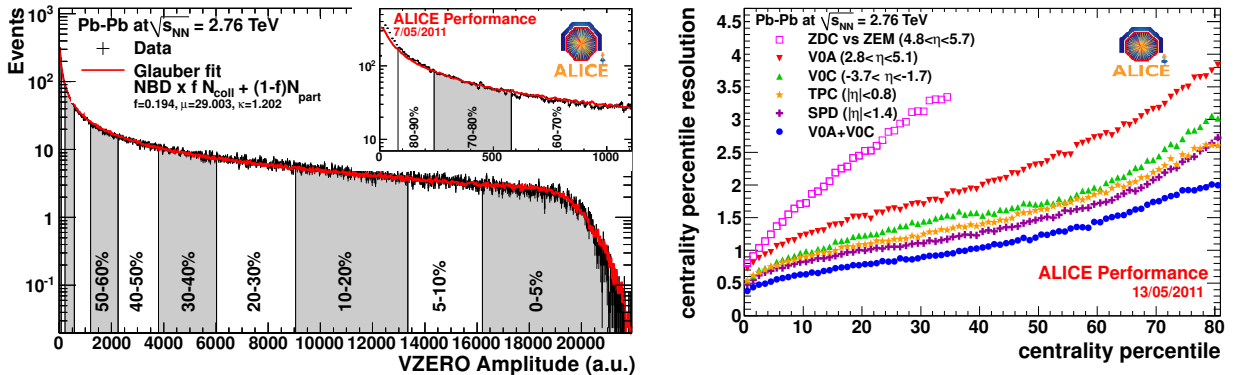


**Figure 6.** Centrality determination in ALICE. Glauber model fit to the VZERO amplitude with the inset of a zoom of the most peripheral region (left); Centrality resolution with different detectors (right).

One of the key observable in heavy ion collision is the charged particle multiplicity and

its dependence on the collision centrality. The main detector used for this measurements in the Silicon Pixel Detector (SPD), two innermost layers of the barrel tracking system covering the pseudorapidity range  $|\eta| < 1.4$ . The charged particle density, normalized to the average number of participants in a given centrality class,  $dN_{\text{ch}}/d\eta / (\langle N_{\text{part}} \rangle)$  was measured by ALICE in PbPb collisions at  $\sqrt{s_{NN}} = 2.76$  TeV and compared with similar measurements at lower energies at RHIC and SPS (Fig.7, left plot) [7]. In the most central events (centrality

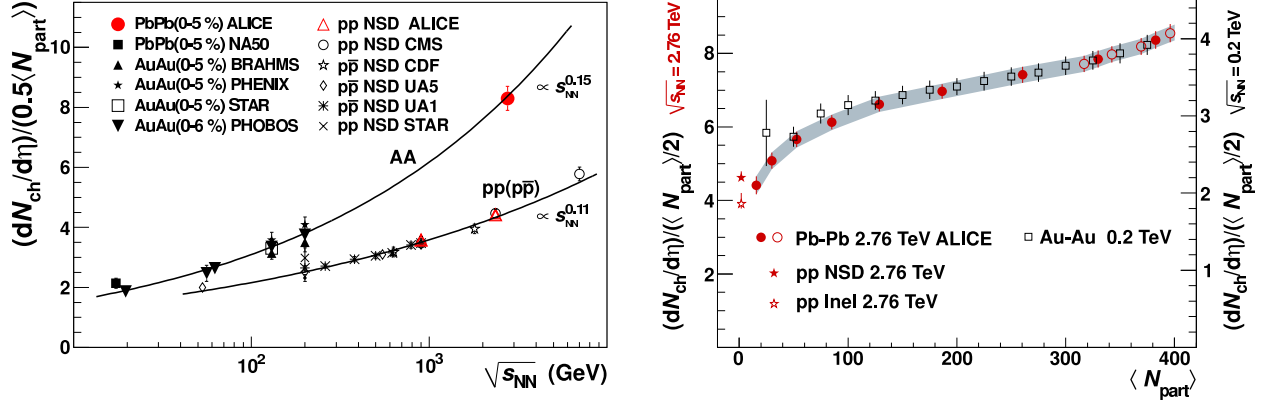


**Figure 7.** Charged track density  $dN/d\eta$  in pp and AA collisions vs collision energy (left) and vs the number of participants (right).

0–5%) at LHC energy the charged particle density was found to be  $dN_{\text{ch}}/d\eta = 1601 \pm 60$  [6] which is, being normalized to the number of participants, is 2.1 times larger than the charged particle density measured at RHIC at  $\sqrt{s_{NN}} = 200$  GeV and 1.9 times larger than that in pp collisions at  $\sqrt{s} = 2.36$  TeV. The dependence of  $dN_{\text{ch}}/d\eta$  on the number of participants  $N_{\text{part}}$ , shown in the right plot of Fig.7, is very similar at LHC ( $\sqrt{s_{NN}} = 2.76$  TeV) and RHIC ( $\sqrt{s_{NN}} = 0.2$  TeV) energies, provided the RHIC points are scaled by a factor 2.1 to match the LHC points.

Longitudinal and transverse expansion of the highly compressed strongly-interacting system created in heavy-ion collisions can be studied experimentally via intensity interferometry, the Bose-Einstein enhancement of identical bosons emitted close by in phase space, known as Hanbury Brown-Twiss analysis (HBT). ALICE has measured the HBT radii and evaluate space-time properties on the system generated in Pb-Pb collisions at  $\sqrt{s_{NN}} = 2.76$  TeV [8]. The two-particle correlation function of the difference  $\vec{q}$  of two 3-momenta  $\vec{p}_1$  and  $\vec{p}_2$  was measured for like-sign charged pions which allowed to get the Gaussian HBT radii,  $R_{\text{out}}$ ,  $R_{\text{side}}$  and  $R_{\text{long}}$ . The product of these 3 radii and decoupling time extracted from  $R_{\text{long}}$ , measured

by ALICE at LHC energy, together with this value measured at the AGS, SPS and RHIC, is shown in Fig.8 (left) as a function of charged track density  $dN_{\text{ch}}/d\eta$ . This measurements

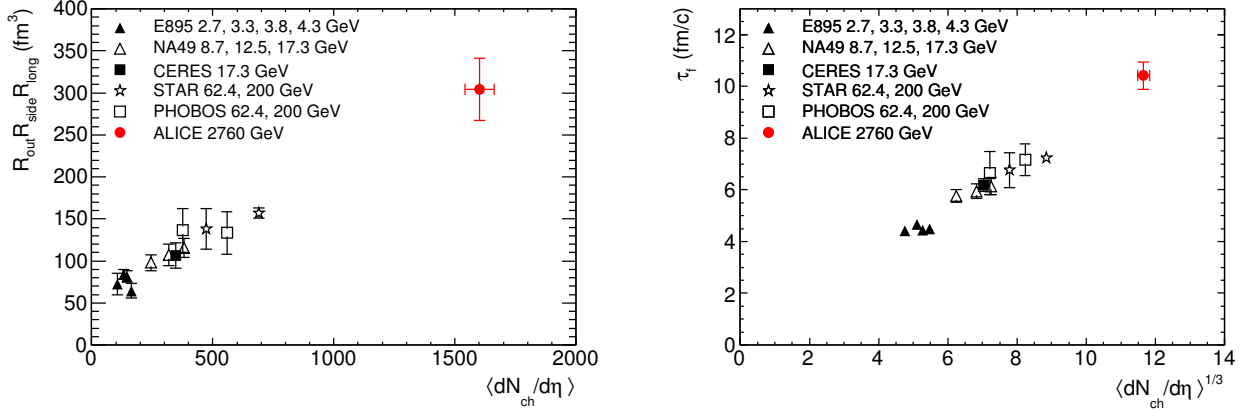


**Figure 8.** System size (left) and lifetime (right).

indicate that the homogeneity volume in central PbPb collisions at  $\sqrt{s_{NN}} = 2.76$  TeV exceeds that measured at RHIC by a factor of 2. The increase is present in both longitudinal and transverse radii. The decoupling time for mid-rapidity pions exceeds 10  $\text{fm}/c$  which is 40% larger than at RHIC (Fig.8, right).

### 3.2. Collective expansion

In non-central collision of nuclei, the overlap region, and hence the initial matter distribution is anisotropic. During evolution of the matter, the spatial asymmetry of initial state is converted to an anisotropic momentum distribution. The azimuthal distribution of the particle yield can be expressed in terms of the angle between the particle direction  $\varphi$  and the reaction plane  $\Psi_{\text{RP}}$ :

$$\frac{dN}{d(\varphi - \Psi_{\text{RP}})} \propto 1 + 2 \sum_{n=1} v_n \cos [n(\varphi - \Psi_{\text{RP}})], \quad (2)$$

$$v_2 = \langle \cos [n(\varphi - \Psi_{\text{RP}})] \rangle. \quad (3)$$

The second coefficient of this Fourier series,  $v_2$ , is referred to as elliptic flow. Theoretical models, based on relativistic hydrodynamics [11, 12], successfully described the elliptic flow observed at RHIC [9] and predict its increase at LHC energies from 10% to 30%.

The first measurements of elliptic flow of charged particles in Pb-Pb collisions at  $\sqrt{s_{NN}} = 2.76$  TeV were reported by ALICE in [10]. Charged tracks were detected and reconstructed

in the central barrel tracking system, consisting of ITS and TPC. Elliptic flow integrated over  $p_t$  range  $0.2 < p_t < 5$  GeV/ $c$ , for the 2- and 4-particle cumulant methods, is shown in Fig.9 (left) as a function of centrality. It shows that the integrated elliptic flow increases

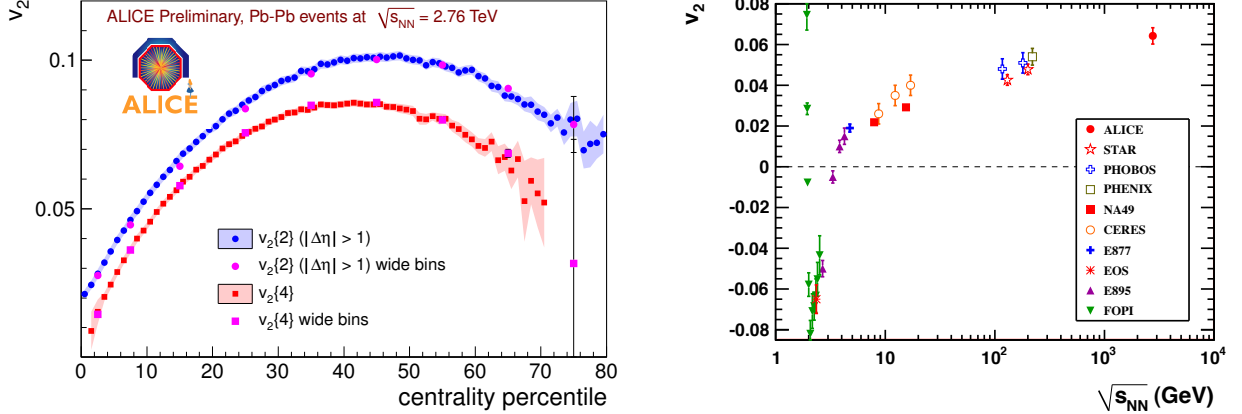


**Figure 9.** Azimuthal flow  $v_2$  of charged particles in Pb-Pb collisions at  $\sqrt{s_{NN}} = 2.76$  TeV vs centrality (left) and  $v_2$  vs collision energy (right).

from central to peripheral collision and reaches the maximum value  $v_2 \approx 0.1$  in semi-central collisions in the 40–60% centrality class. Comparison of the integrated elliptic flow of charged particles, measured at different center-mass collision energies, shows a smooth increase of  $v_2$  with  $\sqrt{s_{NN}}$ , and confirms model expectations that the value of  $v_2$  in Pb-Pb collisions at  $\sqrt{s_{NN}} = 2.76$  TeV increases by about 30% with respect to  $v_2$  in Au-Au collisions at  $\sqrt{s_{NN}} = 0.2$  TeV.

Particle momentum anisotropy is also studied via two-particle correlations which measure the distributions of azimuthal angles  $\Delta\varphi$  and pseudorapidities  $\Delta\eta$  between a “trigger” particle at transverse momentum  $p_t^t$  and an “associated” particle at  $p_t^a$ . The correlation function  $C(\Delta\varphi, \Delta\eta)$  looks differently in different kinematic regions. At  $p_t^t < 3-4$  GeV/ $c$ , the shape of the correlation function reveals the “bulk-dominated” regime, where hydrodynamic modeling has been demonstrated to give a good description of the data from heavy-ion collisions (see Fig.10, left). At high transverse momenta of both particles, jets become dominating, and the shape of the correlation function in central Pb-Pb collisions has just a clear near-side peak centered at  $\Delta\varphi = \Delta\eta = 0$  and no evident out-side peak, as shown in Fig.10, right. Harmonic decomposition of two-particle correlations [13] performed by ALICE, has shown that in the “bulk-dominated” regime a distinct near-side ridge and a doubly-peaked away-side structure are observed in the most central events, which reflects a collective response to anisotropic

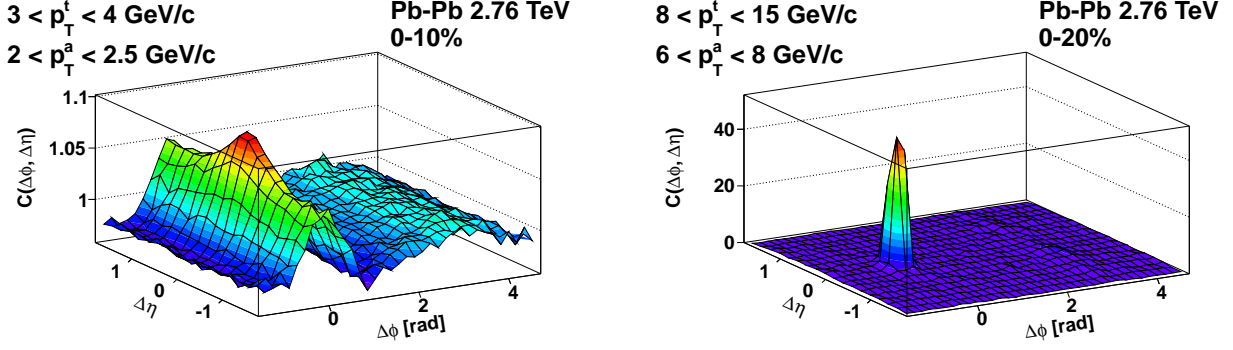


**Figure 10.** Di-hadron correlations  $C(\Delta\varphi, \Delta\eta)$  in central Pb-Pb collisions in the “bult-dominated” regime (left) and in the “jet-dominated” regime (right).

initial conditions.

The results of global event properties and collective expansion studied by ALICE, indicate that the fireball formed in nuclear collisions at the LHC is hotter, lives longer, and expands to a larger size at freeze-out as compared to lower energies.

### 3.3. Strangeness production

Strange particle production has been considered as a probe of strongly interacting matter by heavy-ion experiments at AGS, SPS and RHIC. We have already demonstrated that ALICE, due to its powerful particle identification technique, has measured strange particle spectra in pp collisions. Similar analysis was performed on the Pb-Pb data collected in 2010. Comparison of strange meson and baryon production is illustrated by the  $\Lambda/K_S^0$  ratio measured by ALICE in different centrality classes (Fig.11, left). This ratio in peripheral Pb-Pb collision is similar to that one measured in pp collisions, but it grows with centrality, increasing the value of 1.5 in the most central collisions. The qualitative behaviour of this ratio on  $p_t$  at the LHC collision energy is similar to the ratio measured at RHIC by the STAR experiment (Fig.11, right). An enhancement of strange and multi-strange baryons ( $\Omega^-$ ,  $\bar{\Omega}^+$ ,  $\Sigma^-$ ,  $\bar{\Sigma}^+$ ) was observed in heavy-ion collisions by experiments at lower energies, and was confirmed by ALICE at LHC energy [14]. It was also shown that multi-strange baryon enhancement scales with the number of participants  $N_{\text{part}}$  and decreases with the collision energy.

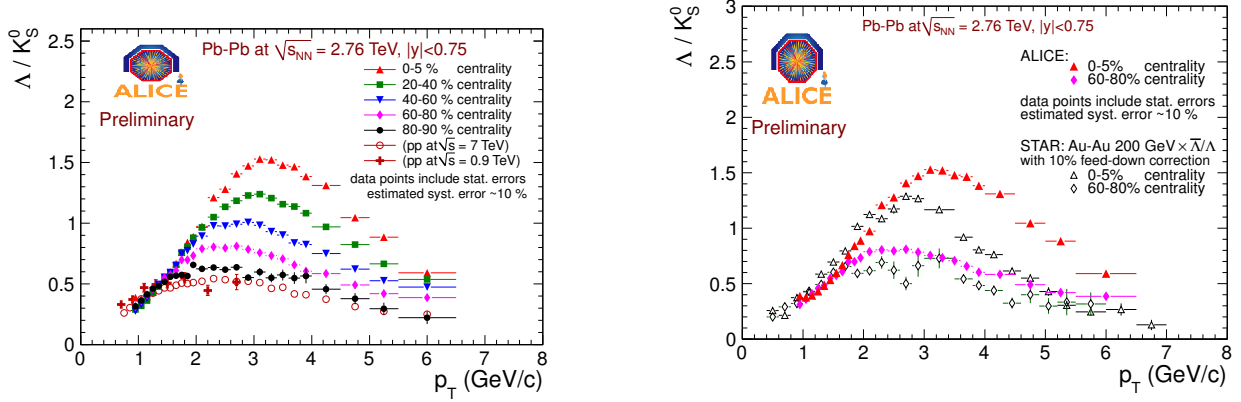


**Figure 11.** Ratio  $\Lambda/K_S^0$  in Pb-Pb collisions at  $\sqrt{s_{NN}} = 2.76$  TeV in different centralities (left) and comparison of this ratio at LHC and RHIC in centralities 0 – 5% and 60 – 80% (right).

### 3.4. Parton energy loss in medium

Experiments at RHIC reported that hadron production at high transverse momentum in central Au-Au collisions at a center-of-mass energy per nucleon pair  $\sqrt{s_{NN}} = 200$  GeV is suppressed by a factor 4 – 5 compared to expectations from an independent superposition of nucleon-nucleon collisions. This suppression is attributed to energy loss of hard partons as they propagate through the hot and dense QCD medium. Therefore, a spectrum suppression of hadron production can be used as a measure of the properties of the strongly interacting matter.

The strength of suppression of a hadron  $h$  is expressed by the nuclear modification factor  $R_{AA}$ , defined as a ratio of the particle spectrum in heavy-ion collision to that in pp, scaled by the number of binary nucleon-nucleon collisions  $N_{\text{coll}}$ :

$$R_{AA}(p_t) = \frac{(1/N_{AA})d^2N_h^{AA}/dp_t d\eta}{N_{\text{coll}}(1/N_{pp})d^2N_h^{pp}/dp_t d\eta}. \quad (4)$$

At the larger LHC energy, the density of the medium is expected to be higher than at RHIC, leading to a larger energy loss of high- $p_t$  partons. However, the hadron production spectra are less steeply falling with  $p_t$  at LHC than at RHIC which would reduce the value of  $R_{AA}$  for a given value of the parton energy loss.

ALICE has measured the nuclear modification factor  $R_{AA}$  for many particles. All charged particles, detected in the ALICE central tracking system (ITS and TPC), show a spectrum suppression [15] which is qualitatively similar to that observed at RHIC (Fig.12). However, quantitative comparison with RHIC demonstrates that the suppression at LHC energy is

stronger which can be interpreted by a denser medium. Benefiting from particle identification

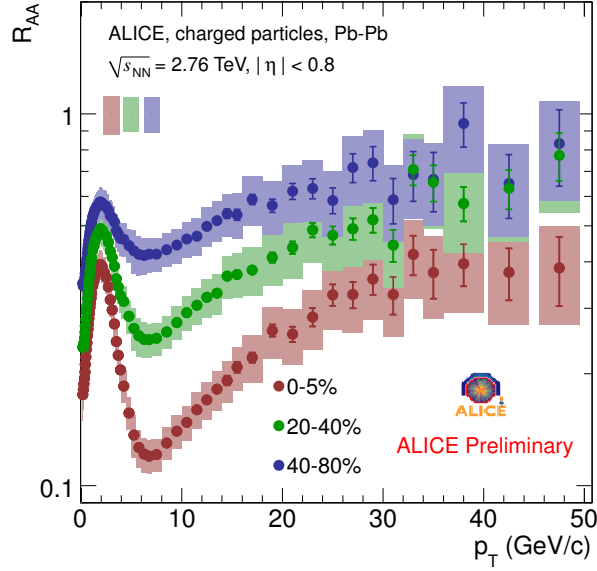


**Figure 12.** Nuclear modification factor  $R_{AA}$  of charged particles.

which has been already mention earlier in this paper, ALICE has measured suppression of various identified hadrons, which provides experimental data for studying the flavor and mass dependence of the spectra suppression.

A nuclear modification factor  $R_{AA}$  of charged pion production in mid-rapidity (Fig.13) has lower values in the range of moderate transverse momenta ( $3 < p_t < 7 - 10$  GeV/c) than that of unidentified charged particles, but at higher  $p_t$  it coincides with all charged particles. To the contrary to charged pions, strange hadrons ( $K_S^0$ ,  $\Lambda$ ) are less suppressed in the most central collisions compared to all charged particles (Fig.14). This is explained by the fact that strange quark production is enhanced in a hot nuclear medium, and this strangeness enhancement partially compensates energy loss of strange quarks, such that the overall  $R_{AA}$  value becomes larger than for pions. Lambda hyperons have no suppression at  $p_t < 3 - 4$  GeV/c, which is interpreted by an additional baryon enhancement in central heavy-ion collisions.

ALICE has reported also the first measurements of  $D$  meson suppression [16] in Pb-Pb collisions in two centrality classes, 0 – 20% and 40 – 80%, shown in Fig.14. It was shown that the  $R_{AA}$  values for  $D^0$ ,  $D^+$  and  $D^{*+}$  are consistent with each other within the statistical and systematical uncertainties. Although the statistics of the ALICE run 2010 is marginal for  $D$  meson measurement, the obtained result shows a hint that the  $D$  mesons are less suppressed

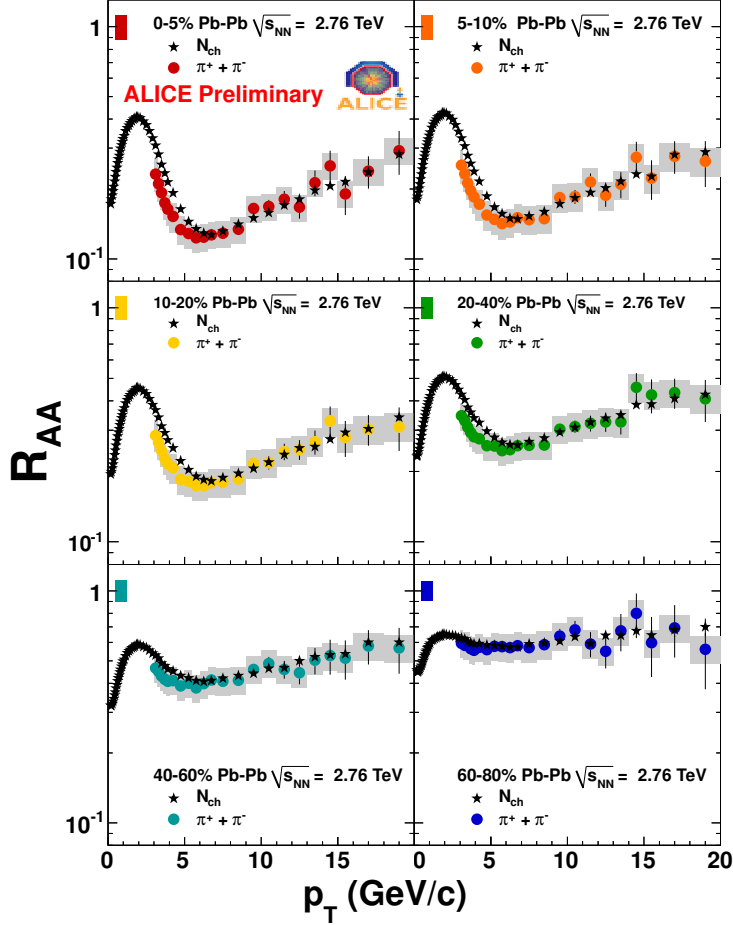


**Figure 13.** Nuclear modification factor  $R_{AA}$  of charged pions.

than charged pions.

#### 4. CONCLUSION

The ALICE collaboration is running an extensive research program with proton-proton collisions. The domain where ALICE is competitive with other LHC experiments, covers event characterization and identified particle spectra at low and medium transverse momenta. Practically all measured spectra in pp collisions at  $\sqrt{s} = 7$  TeV show statistically significant deviations from models which well described lower-energy results. Therefore new experimental results from pp collision allow to tune various phenomenological models and pQCD calculations.

A plenty of experimental results produced by the ALICE collaboration from the first

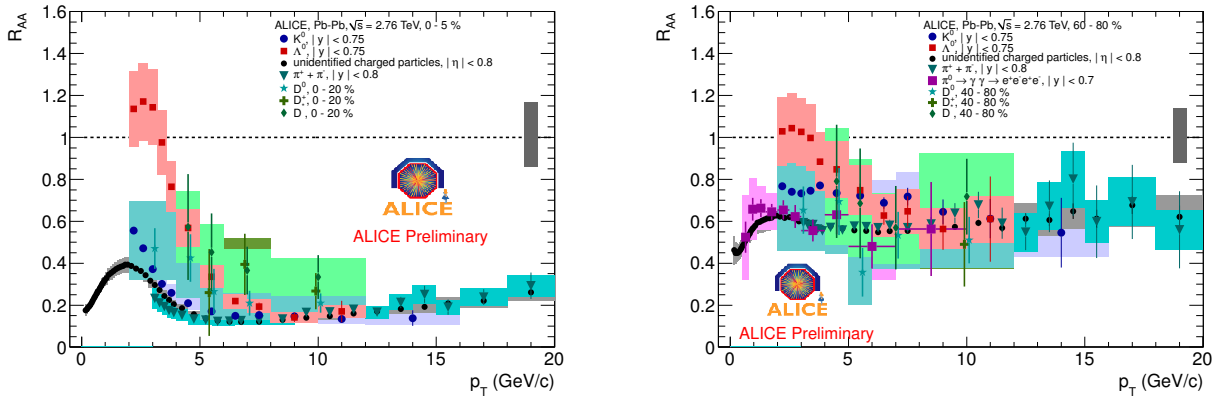


**Figure 14.** Nuclear modification factor  $R_{AA}$  of charged particles,  $K^0$ ,  $\Lambda$ ,  $\pi^\pm$ ,  $D^+$ ,  $D^0$ ,  $D^{*+}$  in central (left) and peripheral (right) collisions.

Pb-Pb data gives the first insight on strongly interacting nuclear matter at the highest achievable collision energy. It is evident that the quark-gluon matter produced in heavy ion collision at LHC qualitatively has properties similar to what was observed at RHIC. The matter produced at LHC has about 3 times larger energy density, twice larger volume of homogeneity and about 20% larger lifetime. Like at RHIC, the matter at LHC reveals the properties on an almost perfect liquid. Particle suppression appeared to be stronger at LHC than at RHIC which is also an evidence of denser medium produced at LHC. At the end of 2011, LHC has delivered 10 times more data with Pb-Pb collision at  $\sqrt{s_{NN}} = 2.76$  TeV, which will bring more precise results.

- 
1. K. Aamodt *et al.* [ALICE Collaboration], JINST **3**, S08002 (2008).
  2. K. Aamodt *et al.* [ALICE Collaboration], Eur.Phys.J.C 71(6), 1655, 2011.
  3. R. Preghenella, for the ALICE Collaboration. arXiv:1111.7080v1 [hep-ex].
  4. C. Tsallis, J. Statist. Phys. **52**, 479-487 (1988).
  5. ALICE collaboration, CERN-PH-EP-2012-001 (2012).
  6. K.Aamodt et al., ALICE collaboration. Phys.Rev.Lett., 106, 032301 (2011).
  7. A.Toia for the ALICE collaboration. J. Phys. G: Nucl. Part. Phys. 38 (2011) 124007.
  8. K.Aamodt et al., ALICE collaboration. Physics Letters B 696 (2011) 328TAY337.
  9. G. Kestin and U.W. Heinz, Eur. Phys. J. C 61, 545 (2009).

10. K.Aamodt et al., ALICE collaboration. *Phys.Rev.Lett.*, 105, 252302 (2010).
11. G. Kestin and U.W. Heinz, *Eur. Phys. J. C* 61, 545 (2009).
12. H. Niemi, K. J. Eskola, and P.V. Ruuskanen, *Phys. Rev. C* 79, 024903 (2009).
13. K.Aamodt et al., ALICE collaboration. arXiv:1109.2501
14. B.Hippolyte for the ALICE collaboration. arXiv:1112.5803 [nucl-ex].
15. J. Otwinowski [ALICE Collaboration], *J. Phys. G* **38** (2011) 124112 [arXiv:1110.2985 [hep-ex]].
16. A.Grelli for the ALICE collaboration. *J. Phys. Conf. Ser.* **316** (2011) 012025.